American Mineralogist, Volume 71, pages 1366–1371, 1986

Heat capacities and entropies of andalusite and sillimanite: The influence of fibrolitization on the phase diagram of the Al_2SiO_5 polymorphs

EKHARD SALJE
Department of Earth Sciences, University of Cambridge, Downing Street, Cambridge CB2 3EQ, England

ABSTRACT

The thermodynamic equilibrium between sillimanite and andalusite has been redetermined from new heat-capacity measurements on andalusite and different samples of sillimanite. Drastic differences are found for bulky "sillimanite" and "fibrolitic" material. Whereas the phase diagram of "sillimanite" is in agreement with the experimental brackets of Holdaway (1971), that of "fibrolite" is closer to the results of Richardson et al. (1969). The enhanced heat capacities of fibrolite as compared with sillimanite are discussed in terms of possible lattice faults in fibrolite that are dominant relative to the role of metallic impurities, Al-Si disorder, or nonstoichiometric Al/Si ratio in the samples investigated.

INTRODUCTION

Although the phase diagram of the Al_2SiO_5 polymorphs, andalusite, sillimanite and kyanite, is commonly used by petrologists for establishing a quantitative grid for metamorphic petrology, uncertainties remain concerning the physical and chemical conditions under which phase equilibria are encountered in nature. The location of the phase equilibrium andalusite-sillimanite in the P-T diagram is especially sensitive to variations of the Gibbs energies of both phases (e.g., because of defects, impurities, etc.). Salje and Werneke (1982a) showed that a small variation of the Gibbs energy by, say, $\partial G = 80$ J/mol for one of these phases changes the resulting triple point of the aluminum silicates in the P-T diagram by $\Delta P = 600$ bars and $\Delta T = 120$ K.

It is possible, therefore, that most phase equilibria, which were determined from the observation of the transformation behavior on a laboratory scale (e.g., Althaus, 1967; Richardson et al., 1969; Holdaway, 1971), represent true equilibria only for the material under investigation. It is not clear, a priori, how far these results are then applicable to real conditions in nature.

In a different experimental approach, Salje and Werneke (1982a) determined the phase equilibrium andalusite-sillimanite using spectroscopic methods. From the observed and calculated lattice vibrations, they approximated the phonon density of states $g(\omega)$ and predicted the temperature dependence of the heat capacities. Their method was first reported by Salje and Viswanathan (1976) and reviewed by Salje and Werneke (1982b). The resulting phase diagram was similar to that of Holdaway (1971). As their approach is principally independent of defect structures, it puts emphasis on the phase diagram of Holdaway as being that of "pure" phases.

The largest uncertainty in the approach of Salje and Werneke concerns the prediction of heat capacities at low temperatures. In the meantime, Robie and Hemingway (1984) have measured the heat capacities of andalusite and sillimanite in the temperature range between ~10 and 300 K. The agreement between the anticipated heat capacities and the observed ones is excellent for sillimanite at temperatures above 80 K (within 1%). At lower temperatures, Robie and Hemingway (1984) found nonrealistic Debye temperatures and attributed this to wrong C_P data due to Fe impurities in their sillimanite sample. For andalusite the agreement between the predicted and measured heat capacities is rather good (better than 2%). However, this difference is too large for further thermodynamic calculations, and the C_P values of Salje and Werneke (1982a) on andalusite (their table 3 for $T < 300$ K) will not be used in the following.

At temperatures above room temperatures, only the heat-capacity data of Pankratz and Kelley (1964) are known. In order to establish the phase boundary between andalusite and sillimanite from heat-capacity measurements and to compare these data with the predicted data, it appeared necessary to redetermine C_P on different, well-characterized samples of andalusite and sillimanite. It is the purpose of this paper to present the experimental results and to calculate the phase equilibrium andalusite-sillimanite using these data, together with those of Robie and Hemingway (1984) and Salje and Werneke (1982a).

MATERIALS, SAMPLE PREPARATION, AND EXPERIMENTAL RESULTS

The heat-capacity measurements on andalusite were performed on a single crystal from the Sta. Teresinka mine, Espirito Santo, Brazil; a chemical analysis was published by Abs-Wurm-

0003–004X/86/1112–1366$02.00

Table 1. Chemical composition (wt%) and lattice constants (Å) of the samples used for DSC impurity contents

Sample	Al/Si ratio	Fe	Cr	Mn	Ti	a_0 (Å)	b_0 (Å)	c_0 (Å)
Sillimanite 1—Harcujuela (Spain)	2.006	0.16	0.08	0.01	0.02	7.4813(17)	7.6739(18)	5.7673(17)
Sillimanite 2—Träskbole (Finland)	1.989	0.35	<0.01	—	0.02	7.4809(23)	7.6664(27)	5.7662(23)
Sillimanite 3—Waldeck (Germany)	2.001	0.08	0.04	<0.01	<0.01	7.4858(22)	7.6647(25)	5.7696(19)
Andalusite Espirito Santo—(Brazil; Abs-Wurmbach and Langer, 1975)	—	0.034	—	<0.001	—	7.796(1)	7.897(1)	5.557(2)

bach and Langer (1975). For the investigation of sillimanite, coarse-grained material from six different localities was prepared. In addition, one single crystal of gem quality from Sri Lanka was used. The powder samples were separated using heavy liquids and by magnetic separation. After each step in the separation process, the samples were checked for purity by powder X-ray diffraction. After this procedure, only three powder samples and the single crystal turned out to be of sufficient purity for further investigation. Chemical analyses of these samples were obtained with an electron microprobe (Camibac system) and are given in Table 1 along with lattice parameters. The samples from Waldeck (Germany) and Harcujuela (Spain) show an Al/Si ratio of 2, within experimental error; the sample from Träskbole (Finland) is slightly Al deficient. The major impurity for all the samples is Fe with a maximum of 0.35 wt% in the sillimanite from Träskbole.

All the purified samples were then examined in a transmission electron microscope (TEM). Two different types of crystals were observed:

1. The samples from Waldeck, Träskbole, and Sri Lanka contained bulky crystals with idiomorphic habit. Some grains were ion-milled and investigated at higher magnifications. These were fully homogeneous and contained very few dislocations. No evidence of extended defect structures was found. The TEM images are identical to the results of Menard and Doukhan (1978).

2. The samples from Harcujuela contain fibrolitic material with intergrowths of fine needles forming thicker columns. In very rare cases, grains contained a few small platelets of biotite so completely intergrown that no separation could be achieved with the techniques mentioned above.

In the fibrolitic material, Cameron and Ashworth (1972) reported the appearance of diffuse streaks in electron diffraction of *hkl*: $l = 2n + 1$, similar to the observations of Smith and McConnell (1966) on mullite. No such diffuse scattering was found in our specimen, and no indication for an additional mullite phase appears from these observations. The only weak diffuse diffracted intensity in the electron-diffraction pattern occurred in the (001) plane and is presumably due to stacking faults with Burgers vectors of [0, 0, c/2].

The heat-capacity measurements were made using a modified Perkin-Elmer calorimeter (DSC 2). The weights of the powdered samples were between 40 and 60 mg; the measuring procedure has been described in detail by Salje and Wruck (1983). Each datum for the powders was measured independently eight times, and the standard deviation is below 1%. The heat capacity of the single crystal was measured 20 times at each temperature, and the standard deviation was found to be 2.5%. This large value is due to the small weight of the sample (3.532 mg) compared with the powdered samples. The experimental results are listed in Table 2 and are shown graphically in Figure 1.

In a separate experiment, the influence of the crystallinity (or the grain surface) was tested on coarse-grained sillimanite from Träskbole. The heat capacities were first measured in a separate experiment using a coarse crystal. Subsequently, part of the sample was ground to a fine powder using a spex-mill. The grinding procedure was continued until the X-ray powder lines started to widen, which indicates a grain size of ~400 Å. The fine powder was then annealed at 900 K for 1 d in order to remove volatile surface contamination. The heat capacities of the annealed powder were then measured again in ten independent runs. No systematic changes during these ten different runs were observed. The resulting averaged heat capacities are shown graphically in Figure 2.

The phase equilibrium andalusite-sillimanite

All the sillimanite samples under investigation were of extremely high purity, and the differences between their heat capacities in Figure 1 cannot be attributed to the presence of traces of other mineral phases. It is therefore necessary to assume that different crystals of sillimanite possess different heat capacities and, consequently, different thermodynamic stabilities. The open questions are, then, what is the influence of these differences on the location of the phase equilibrium andalusite-sillimanite in the P-T field, and, how one can explain the different C_P-values of sillimanite on an atomistic level? The influence on the P-T conditions for the phase equilibrium is discussed first.

Table 2. Heat capacities of one andalusite and four sillimanites in J/(mol·K)

T (K)	1	2	3	4	5
380	146.6	146.1	145.9	142.1	147.7
385	147.7	146.6	147.1	142.8	148.4
390	148.7	147.6	147.9	144.1	149.3
395	149.8	148.4	148.6	144.4	150.0
400	150.7	148.8	149.6	145.4	151.1
405	151.7	149.9	151.1	146.7	151.9
410	152.6	150.6	151.5	147.2	152.8
415	153.6	151.7	152.0	147.3	153.8
420	154.4	152.4	153.3	147.5	154.7
425	155.3	153.1	154.2	148.6	155.9
430	156.2	154.0	155.3	149.6	156.4
435	157.0	155.0	155.8	150.4	157.2
440	157.8	155.6	156.5	151.3	158.0
445	158.7	156.4	157.6	152.2	158.9
450	159.4	157.5	157.9	153.1	159.9
455	160.2	157.8	158.8	153.6	160.5
460	160.9	158.6	158.9	156.8	161.1
465	161.7	159.3	160.0	157.5	161.8
470	162.4	160.0	161.4	156.0	162.8
475	163.1	160.5	161.7	157.2	163.6
480	163.8	161.3	162.1	158.0	164.4
485	164.4	162.3	162.4	158.8	165.3

Note: Columns are (1) andalusite (Espirito Santo) and (2–5) sillimanite—(2) Waldeck, (3) Träskbole, (4) Sri Lanka, (5) Harcujuela.

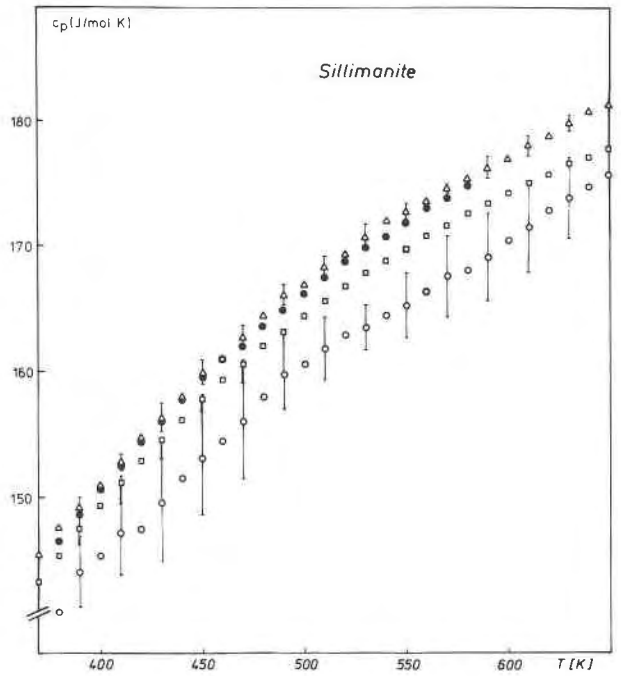

Fig. 1. Heat capacities of sillimanite and andalusite (●). The sillimanite samples are listed in Table 1: Sri Lanka (○), Waldeck (□) and Harcujuela (△). The heat capacities of sillimanite from Träskbole are very close to those of Waldeck and could not be distinguished on this scale. Typical experimental standard deviations are shown as brackets. The standard deviations of andalusite are the diameters of the ● symbols.

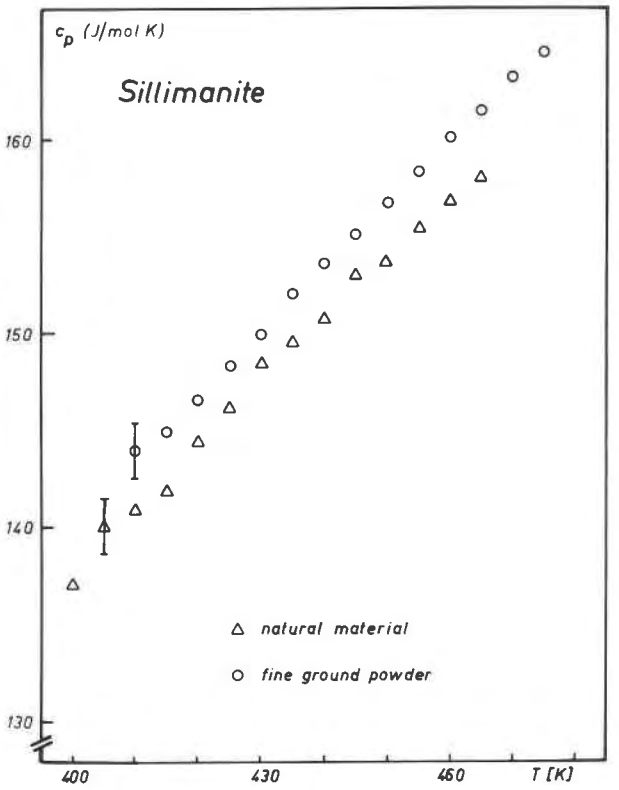

Fig. 2. Heat capacities of sillimanite from Träskbole before (△) and after grinding (○).

The heat-capacity data in Table 2 were expressed using a polynomial approach

$$C_P = a + bT + CT^{+2} + dT^{-1/2} + eT^{-2}. \qquad (1)$$

The coefficients were fitted to the experimental data by least-square methods. In agreement with Robie and Hemingway (1984), the T^2 term was found to be not significant and therefore was omitted in the fitting procedure; the linear term turned out to be numerically small. The resulting equations are C_P^0 (andalusite) = 274.002 + $2.5916 \times 10^{-10}T - 2327.85T^{-0.5} - 1\,238\,069.87T^{-2}$ and S_0 (andalusite) = 91.39 J/(mol·K) at T = 298.15 K, C_P^0 (sillimanite, Träskbole) = $237.316 + 1.951 \times 10^{-11}T - 1323.37T^{-0.5} - 3\,366\,105.1T^{-2}$ and S_0 (298.15 K) = 97.07 J/(mol·K), C_P^0 (sillimanite, Sri Lanka) = $286.598 - 6.6755 \times 10^{-11}T - 2845.61T^{-0.5} + 147\,765.47T^{-2}$ and S_0 (298.15 K) = 97.68 J/(mol·K), C_P^0 (sillimanite, Waldeck) = $243.843 + 6.126 \times 10^{-12}T - 1498.94T^{-0.5} - 3\,174\,273.87T^{-2}$ and S_0 (298.15 K) = 97.07 J/(mol·K), and C_P^0 (sillimanite, Harcujuela) = $255.645 + 3.059 \cdot 10^{-12}T - 1717.37T^{-0.5} - 2\,981\,146.23T^{-2}$ and S_0 (298.15 K) = 101.12 J/(mol·K).

The standard entropy of andalusite is taken from Robie and Hemingway (1984). In the case of sillimanite, the standard entropies were obtained using the method of Salje and Werneke (1982b); namely, the phonon densities of states were fitted to give a best fit with the experimental heat capacities at high temperatures. The heat capacities at low temperatures were then calculated using the Debye temperatures determined from the elastic constant data of Vaughan and Weidner (1978) and integrated to obtain the standard entropies. All standard entropies are slightly higher than the value of Robie and Hemingway (1984) which is S_0 = 95.79 J/(mol·K). The difference is mainly due to the anomalously low heat capacities of sillimanite measured by Robie and Hemingway for temperatures below 80 K. For higher temperatures the calculated and measured heat capacities are practically identical.

The entropy at higher temperatures is given by

$$S = \int_{298.15}^{T} \frac{C_P^0}{T}\, dT + S_{298.15}. \qquad (2)$$

The above-mentioned series expansions of C_P^0 are used without further corrections up to temperatures of the andalusite-sillimanite transition (at 1 bar), which takes place at 1049 ± 20 K on the basis of Holdaway's high-pressure reversals and unpublished measurements of Weill as reported by Holdaway (1971). We start with this value and calculate the phase boundary for the equilibrium sillimanite-andalusite using the approximation

$$\int dP\,[V_{A,1048}(1 - \alpha_A T)(1 + \beta_A P) - V_{S,1048}(1 - \alpha_S T)(1 + \beta_S P)] = \int dT\,\Delta S, \qquad (3)$$

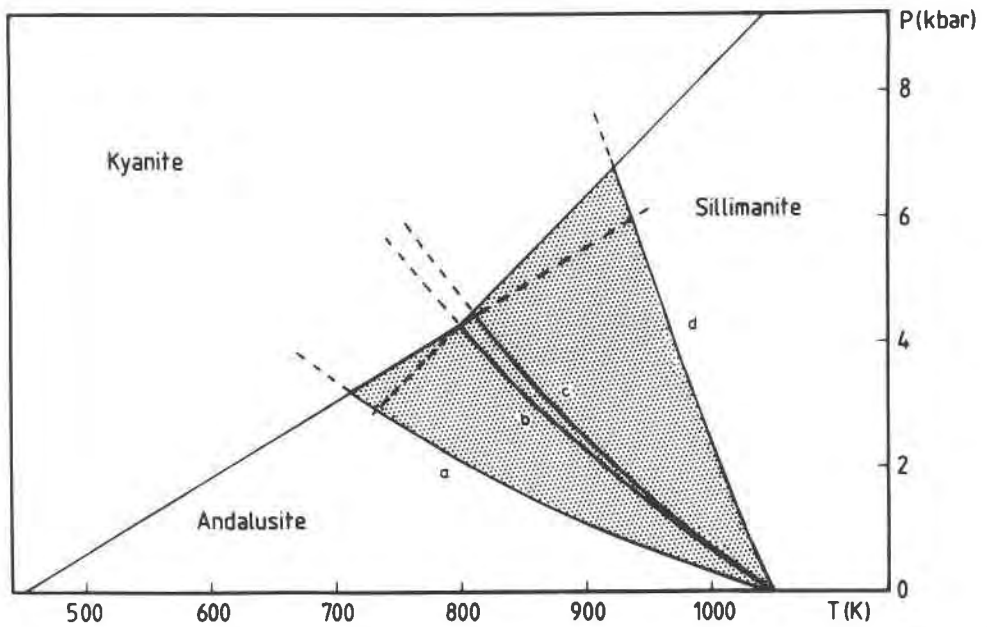

Fig. 3. The triple point for the equilibrium transitions kyanite-sillimanite, kyanite-andalusite, andalusite-sillimanite, i.e., curve *b*, for the andalusite-sillimanite equilibrium as determined for coarse-grained, bulky sillimanite from Waldeck. Curves *a* (Sri Lanka), *c* (Tränskbole), and *d* (Harcujuela) represent andalusite-sillimanite equilibria for bulky material (*a, c*) and fibrolitic needles (*d*). For each of these equilibria there exists a triple point, but for clarity, the phase boundaries kyanite-andalusite and kyanite-sillimanite are not shown for these sillimanite samples (*a, c, d*).

where α is the coefficient of thermal expansion, β is the compressibility, and subscripts S and A represent sillimanite and andalusite, respectively. The resulting P-T curve may be calculated from

$$P = \Delta V_{1048} + \frac{(\alpha_A V_A - \alpha_S V_S)(T - 1048)}{\beta_A V_A - \beta_S V_S} - \left[\frac{(\alpha_A V_A - \alpha_S V_S)(T - 1048)}{\beta_A V_A - \beta_S V_S}\right]^2 - \frac{2}{\beta_A V_A - \beta_S V_S 1048} \int_{1048}^{T} \Delta S \, dT. \quad (4)$$

This equation must be used instead of the oversimplifying Clapeyron equation because the equilibrium boundary cannot be expected to be linear in P-T space (Robie and Hemingway, 1984). The coefficients of thermal expansion are $\alpha_A = 2.46 \times 10^{-5}$ K^{-1}, $\alpha_S = 1.47 \times 10^{-5}$ K^{-1} (Winter and Ghose, 1979). The volume compressibilities were derived from the data of Vaughan and Weidner (1978) and are $\beta_A = 6.0277 \times 10^{-7}$ bar^{-1} and $\beta_S = 5.71 \times 10^{-7}$ bar^{-1}. The molar volumes at $T = 1048$ K are $V_A = 52.82$ cm^3/mol and $V_S = 50.761$ cm^3/mol (Winter and Ghose, 1979). Using these data, the C_P polynomials, and the given standard entropies, Equation 4 was solved numerically. The resulting phase boundaries are shown in Figure 3. Curves *a, b,* and *c* are based on data for coarse-grained sillimanite, and curve *d* is based on fibrolite. The phase boundaries of the Träskbole sillimanite (*c*) and the Waldeck sillimanite (*b*) are almost identical and agree with the phase diagram of Holdaway (1971). The phase boundary of the sillimanite from Sri Lanka (*a*) is the least certain in this investigation because of the large standard deviations of the C_P measurements, but the resulting equilibrium temperatures are at markedly lower values and are outside the estimated error (±20 K). This means that even the triple point for the samples from Träskbole and Waldeck (795 ± 15 K, 4.2 ± 0.2 kbar) or that of Holdaway (774 K, 3.76 kbar) do not represent those of "ideal" sillimanite, which is expected to be at slightly lower temperatures and pressures (715 K, 3.2 kbar).

Differences in the position of the phase equilibrium andalusite-sillimanite and the aluminum silicate triple point discussed so far are much smaller than the difference obtained between bulky and fibrolitic material. The phase equilibrium of the sample from Harcujuela (curve *d* in Fig. 3) is similar to that proposed by Richardson et al. (1969) and leads to a triple point at 936 K and 5.9 kbar.

We are, therefore, dealing with a "transition field" instead of a well-defined "transition line" in the P-T diagram for the phase equilibrium between andalusite and sillimanite. The thermodynamic equilibrium conditions depend very much on the structural state of the material under investigation. This result is independent of the actual numerical values of the standard entropies. Different crystals of chemically pure sillimanite possess different values of C_P^0 at all temperatures examined in this work, and consequently, the standard entropies and their phase stabilities must also vary.

Defect model for fibrolite

The experimental results show that the phase boundary of the andalusite-sillimanite equilibrium becomes steeper in the P-T diagram with increasing "fibrolitization." The Al/Si ratio, on the other hand, seems to have a much smaller influence. This follows from the observation of very similar phase equilibria for Waldeck and Träskbole sillimanite, although their Al/Si ratios vary from 2.006(7) to 1.989(7). The Al/Si ratio of the fibrolitic sample is 2.001(3). The anomalous thermodynamic character of fibrolite is therefore not due either to the Al/Si ratio or to specific metal impurities, as shown by the chemical compositions listed in Table 1.

Another explanation could be based on possible Al-Si disorder in sillimanite. Preliminary neutron-scattering experiments on powder samples gave no indication of any statistical disorder effects, however (Salje and Werneke, 1982a). Furthermore, the possible order-disorder temperature is supposed to be above 2010 K, and the influence on the entropy of sillimanite for temperatures close to 1048 K is expected to be too small to explain the observed differences (Greenwood, 1972; Carpenter, 1985).

The anomalous thermodynamic behavior of fibrolite does not, therefore, correlate with either (1) its chemical composition (Al/Si ratio), (2) specific metallic impurities, or (3) statistical Al-Si disorder. Furthermore, the specific heat, calculated from lattice vibrations by Salje and Werneke (1982a), agrees within less than 1% error with the experimental data on bulky sillimanite. No physically realistic phonon density of state concerning the defect-free crystal could be derived in order to fit the experimental values of fibrolite, which are more than 2% higher than those of bulky sillimanite ($T > 300$ K). It is concluded that defect properties are the probable cause of the increased C_P values of fibrolite rather than systematic changes of phonon frequencies.

A tentative model of a defect structure of fibrolite is based on the stacking faults in sillimanite observed in TEM studies (Menard and Doukhan, 1978; Doukhan et al. 1985; Lefebvre and Paquet, 1983). Dislocations with **c** as Burgers vector are the predominant defects in naturally deformed sillimanite, and they are widely dissociated into two collinear partials **c**/2 in (100) or (010) (Menard and Doukhan, 1978; Lefebvre and Paquet, 1983). A second type of stacking fault, ½ [001] parallel to the (hk0) planes, was observed by Lefebvre and Paquet (1983). When parallel to (100) the stacking faults may be located either along the **b** glide planes of the sillimanite structure or between them. In the first case the Al^{IV}-Si^{IV} ordering of the double chains is not altered. In the second case Al^{IV}-O-Al^{IV} contacts are created and thereby Al-Si disorder is introduced. The observed defect densities can be as high as 5% per unit cell (Lefebvre and Paquet, 1983). It is therefore possible that the enhanced specific heat of fibrolitic material is correlated with higher defect densities in this sample.

Besides the influence of the dislocations and the stacking faults as internal surfaces, the additional influence of further internal and external planes of defects is presumably also important in the case of fibrolite. These "surfaces" are due to intergrowth and grain-size effects of the needle-shaped crystals. The frequencies of the surface-related modes are in general smaller than those of the correlated bulk modes, and we have to expect enhanced heat capacities for samples with large specific internal or external surfaces.

In order to give a first estimate of the grain-size effects, bulky sillimanite was powdered to an averaged grain size of ~400 Å. The differences between the heat capacities of the virgin crystals and the powdered sample (Fig. 2) show an increase of C_P of ~2% due to the grinding procedure. No contamination from the prolonged grinding was found on the sample as judged from X-ray inspection. Although the particle size of 400 Å is smaller than that of typical fibrolite, the tendency of increasing heat capacities due to reduced grain sizes and the imposed strain fields is clearly demonstrated in this experiment. In conclusion, the observed increases in the heat capacities of fibrolite as compared with sillimanite are attributed to lattice faults in fibrolite that occur as internal surfaces (dislocations, stacking faults, intergrowth of needles) or external surfaces (grain-size effects).

Acknowledgments

The author thanks Ch. Werneke and B. Kuscholke for technical assistance. He acknowledges the critical reading of the manuscript and the helpful discussions with M. A. Carpenter. The project was financially supported by the D.F.G. (SFB 173).

References

Abs-Wurmbach, I., and Langer, K. (1975) Synthetic Mn^{3+}-kyanite and viridine, $(Al_{2-x}M^{3x}_x)SiO_5$, in the system Al_2O_3-MnO-MnO_2-SiO_2. Contributions to Mineralogy and Petrology, 49, 21–38.

Althaus, E. (1967) The triple point andalusite-sillimanite-kyanite: An experimental and petrologic study. Contributions to Mineralogy and Petrology, 16, 29–44.

Cameron, W.E., and Ashworth, J.R. (1972) Fibrolite and its relationship to sillimanite. Nature (Physical Sciences), 235, 134–136.

Carpenter, M.A. (1985) Order-disorder transformations in mineral solid solutions. Mineralogical Society of America Reviews in Mineralogy, 14, 187–223.

Doukhan, J.C., Doukhan, N., Koch, P.S., and Christie, J.M. (1985) Transmission electron microscopy investigation of lattice defects in Al_2SiO_5 polymorphs and plasticity induced polymorphic transformations. Bulletin de Minéralogie, 108, 81–96.

Greenwood, H.J. (1972) Al^{IV}-Si^{IV} disorder in sillimanite and its effect on phase relations of the aluminium silicate minerals. Geological Society of America Memoir 132, 553–571.

Holdaway, M.J. (1971) Stability of andalusite and the aluminium silicate phase diagrams. American Journal of Science, 271, 97–131.

Lefebvre, A., and Paquet, J. (1983) Dissociation of c dislocations in sillimanite Al_2SiO_5. Bulletin de Minéralogie, 106, 287–292.

Menard, D., and Doukhan, J.C. (1978) Défects de Rèseau dans la sillimanite Al_2O_3-SiO_2. Journal of Physics Le Hers, 39, L-19–L-22.

Pankratz, L.B., and Kelley, K.K. (1964) High temperature heat

content and entropies of andalusite, kyanite and sillimanite. U.S. Bureau of Mines Report of Investigations 6370.

Richardson, S.W., Gilbert, M.C., and Bell, P.M. (1969) Experimental determination of the kyanite-andalusite and andalusite-sillimanite equilibria; the aluminum silicate triple point. American Journal of Science, 267, 259–272.

Robie, R.A., and Hemingway, B.S. (1984) Entropies of kyanite, andalusite, and sillimanite: Additional constraints on the pressure and temperature of the Al_2SiO_5 triple point. American Mineralogist, 69, 298–306.

Salje, E., and Viswanathan, K. (1976) The phase diagram calcite-aragonite as derived from the crystallographic properties. Contributions to Mineralogy and Petrology, 55, 55–67.

Salje, E., and Werneke, Ch. (1982a) The phase equilibrium between sillimanite and andalusite as determined from lattice vibrations. Contributions to Mineralogy and Petrology, 79, 56–67.

——— (1982b) How to determine phase stabilities from lattice vibrations. In W. Schreyer, Ed. High-pressure researches in geoscience, 321–348. E. Schweizerbart'sche Verlagsbuchhandlung, Stuttgart.

Salje, E., and Wruck, B. (1983) Specific-heat measurements and critical exponents of the ferroelastic phase transition in $Pb_3(PO_4)_2$ and $Pb(P_{1-x}As_xO_4)_2$. Physical Review B, 28, 6510–6518.

Smith, D.G.W., and McConnell, J.D.C. (1966) A comparative electron-diffraction study of sillimanite and some natural and artificial mullites. Mineralogical Magazine, 35, 810–814.

Vaughan, M.T., and Weidner, D.J. (1978) The relationship of elasticity and crystal structure in andalusite and sillimanite. Physics and Chemistry of Minerals, 3, 133–144.

Winter, J.K., and Ghose, S. (1979) Thermal expansion and high-temperature crystal chemistry of the Al_2SiO_5 polymorphs. American Mineralogist, 64, 573–586.

Manuscript received September 11, 1985
Manuscript accepted July 8, 1986